Enhancement of Sputtering Yields Due to C₆₀ versus Ga Bombardment of Ag{111} As Explored by Molecular Dynamics Simulations

Zbigniew Postawa,*,† Bartlomiej Czerwinski,† Marek Szewczyk,† Edward J. Smiley,‡,§ Nicholas Winograd,‡,§ and Barbara J. Garrison*,‡

Smoluchowski Institute of Physics, Jagiellonian University, Krakow, Poland, and 152 Davey Laboratory, Department of Chemistry, and 184 Materials Research Institute, The Pennsylvania State University, University Park, Pennsylvania 16802

The mechanism of enhanced desorption initiated by 15keV C₆₀ cluster ion bombardment of a Ag single crystal surface is examined using molecular dynamics computer simulations. The size of the model microcrystallite of 165 000 atoms and the sophistication of the interaction potential function yields data that should be directly comparable with experiment. The C₆₀ model was chosen since this source is now being used in secondary ion mass spectrometry experiments in many laboratories. The results show that a crater is formed on the Ag surface that is $\sim \! 10$ nm in diameter, a result very similar to that found for Au_3 bombardment of Au. The yield of Ag atoms is ~ 16 times larger than for corresponding atomic bombardment with 15-keV Ga atoms, and the yield of Ag₃ is enhanced by a factor of 35. The essential mechanistic reasons for these differences is that the C₆₀ kinetic energy is deposited closer to the surface, with the deeply penetrating energy propagation occurring via a nondestructive pressure wave. The numbers predicted by the model are testable by experiment, and the approach is extendable to include the study of organic overlayers on metals, a situation of growing importance to the SIMS community.

Cluster ion beams are recognized as valuable sources for desorption of high-mass ions in secondary ion mass spectrometry (SIMS) experiments.^{1–5} Since the initial discovery of their unique power for surface analysis, many different organic and inorganic probes have been evaluated for incorporation into a routine laboratory environment.^{6–9} Their use received a boost about 5

years ago when an SF_5^+ ion source was introduced commercially. This cluster ion source has proven to be a powerful spectroscopic probe, particularly for analysis of organic thin films and polymers. The technology is still not as widely used as it might be, however, since the source is difficult to focus for imaging purposes, and the lifetime is still rather short.

There have recently been reports of two additional cluster beams that overcome lateral resolution and lifetime issues. The first of these utilizes liquid metal ion gun (LMIG) technology,11 commonly employed with Ga⁺ ions, to produce an extremely bright source of Au_3^+ ions that is focusable to less than 100 nm and has a lifetime of more than 500 h. Results from preliminary experiments are quite promising. 12-14 The second source utilizes an improved LMIG design to produce a stable beam of 10-20keV C₆₀ ions at 1 nA that can be pulsed for time-of-flight experiments, can be focused to a probe size approaching $1 \mu m$, and has a lifetime of 500 h.15,16 As suggested by earlier experiments,4 this projectile exhibits remarkable performance. The yield of the peptide gramicidin, for example, is enhanced by a factor of 1300 when compared to Ga⁺ ion bombardment.¹⁵ There are even indications that there is minimal accumulation of beam-induced damage on the surface of the material, opening the possibility of molecular depth-profiling experiments.

The reasons behind the unique properties of cluster ion beams are still not well-understood. Various degrees of enhancement of high-mass secondary ions have been reported, depending upon the type of projectile, target material, and matrix.¹⁰ For example, thin polymer films on Ag do not seem to benefit from the use of polyatomic projectiles, while SIMS spectra from bulk polymers

^{*} Corresponding authors. E-mail: zp@castor.if.uj.edu.pl; (4812) 632-4888 ext 5626. E-mail: bjg@psu.edu. Phone: 814-863-2103.

[†] Jagiellonian University.

[‡] Department of Chemistry, The Pennsylvania State University.

^{§ 184} Materials Research Institute, The Pennsylvania State University.

⁽¹⁾ Castner, D. G. Nature 2003, 422, 122.

⁽²⁾ Applehans, A. D.; Delmore, J. E. Anal. Chem. 1989, 61, 1087.

⁽³⁾ Blain, M. G.; Della-Negra, S.; Joret, H.; Le Beyec, Y.; Schweikert, E. A. Phys. Rev. Lett. 1989, 63, 1625.

⁽⁴⁾ Van Stipdonk, M. J.; Harris, R. D.; Schweikert E. A. Rapid Commun. Mass Spectrom. 1996, 10, 1987.

⁽⁵⁾ Takeuchi, D.; Seki, T.; Aoki, T.; Matsuo J.; Yamada, I. Mater. Chem. Phys. 1998, 54, 76.

⁽⁶⁾ Mahoney, J. F.; Perel, J.; Ruatta, S. A.; Martine, P. A.; Husain, S.; Lee, T. D. Rapid Commun. Mass Spectrom. 1991, 5, 441.

⁽⁷⁾ Gillen, G.; Robertson, S. Rapid Commun. Mass Spectrom. 1998, 12, 1303.

⁽⁸⁾ Gillen, G.; King, L.; Freibaum, B.; Lareau, R.; Bennett, J.; Chmara, F. J. Vac. Sci., Technol. A 2001, 19, 568.

⁽⁹⁾ Fuoco, E. R.; Gillen, G.; Wijesundara, M. B. J.; Wallace, W. E.; Hanley, L. J. Phys. Chem. B 2001, 105, 3950.

⁽¹⁰⁾ Kötter, F.; Benninghoven, A. Appl. Surf. Sci. 1998, 133, 47.

⁽¹¹⁾ Prewett, P. D.; Jefferies, D. K. J. Phys. D: Appl. Phys. 1980, 13, 1747.

⁽¹²⁾ Hagenhoff, B.; Kersting, R.; Rading, D.; Kayser, S.; Niehuis, E. Proceedings of the 12th International Conference on Secondary Ion Mass Spectrometry, Benninghoven, A., Bertrand, P., Migeon, H.-N., Werner, H. W., Eds.; Elsivier: Amsterdam, 2000; p 833.

⁽¹³⁾ Davies, N.; Weibel, D. E.; Blenkinsopp, P.; Lockyer, N.; Hill, R.; Vickerman, J. C. Appl. Surf. Sci. 2003, 203–204, 223.

⁽¹⁴⁾ Walker, A. V.; Winograd, N. Appl. Surf. Sci. 2003, 203-204, 198.

⁽¹⁵⁾ Weibel, D.; Wong, S. C. C.; Lockyer, N.; Blenkinsopp, P.; Hill R.; Vickerman, J. C. Anal. Chem. 2003, 75, 1754–1764

⁽¹⁶⁾ Wong, S. C. C.; Hill, R.; Blenkinsopp, P.; Lockyer, N. P.; Weibel, D. E.; Vickerman, J. C. *Appl. Surf. Sci.*, in press.

are dramatically improved. 10 Theoretical calculations are beginning to unravel some of the complexities. Molecular dynamics (MD) simulations of C_{60} impact with kinetic energy in the range of 10-20 keV on graphite 17,18 and diamond 19 show that a crater forms and that the energy is deposited in the near-surface region. Calculations of small metal cluster bombardment in the same energy range predict similar crater formation on graphite 17 and metal substrates. $^{20-22}$ At lower kinetic energies, it has been shown that the mass of the substrate is important in determining the mechanism of the enhancement effect. 23

To fully understand enhancement of signals in SIMS experiments, we are initiating a comprehensive series of MD investigations aimed at understanding the collision cascades due to the C₆₀ cluster versus the Ga atom projectile on a number of welldefined substrates and for various beam energies and incident angles. In this paper, we discuss molecular dynamics computer simulations aimed at determining enhancement effects of 15-keV C₆₀ bombardment of Ag{111} surfaces compared to bombardment with Ga projectiles. These beams and energies are typical of experimental configurations. The main goal of this paper is to outline a computational strategy for this type of simulation and to present some general predictions that may be useful for application of C₆₀ clusters to perform chemical analysis. With these procedures, it should be possible to utilize MD simulations to investigate thin and thick overlayers of organic molecules on Ag{111} and to extract the essential mechanisms associated with the enhancement effect.

Model Details. The C₆₀ and Ga bombardment of a clean Ag{111} surface is modeled using MD computer simulations since MD simulations provide an excellent representation of particle bombardment events.^{24,25} The MD simulations allow calculation of experimentally observable properties such as total yield, mass distribution of neutral species, kinetic energy, and angular distributions. It is also possible to follow atomic motions in order to obtain microscopic insight. An extensive description of the MD scheme can be found elsewhere.^{24,26}

The forces among the atoms are described by a blend of empirical pairwise additive and many-body potential energy functions. The Ag-Ag interactions are described by the molecular dynamics/Monte Carlo-corrected effective medium (MD/MC-CEM) potential for fcc metals.²⁷ The Ga-Ag interactions are described using the purely repulsive Moliére pairwise additive potential. The adaptive intermolecular potential, AIREBO, devel-

oped by Stuart and co-workers is used to describe the C-C interactions. ²⁸ This potential is based on the reactive empirical bond-order (REBO) potential developed by Brenner for hydrocarbon molecules. ^{29,30} The AIREBO potential yields a binding energy per atom in the relaxed C_{60} cluster of 7.2 eV, which compares well with the experimental value of 7.4 eV. ³¹ Finally, the interaction between C and Ag atoms is described by a Lennard-Jones potential with parameters given in ref 32.

Our model approximating the Ag{111} substrate consists of a finite microcrystallite containing 166 530 atoms arranged in 39 layers of 4270 atoms each. The sample size (175 \times 174.5 \times 89.7 Å) was chosen to minimize edge effects on the dynamical events leading to ejection of particles. Projectiles of 15-keV Ga and C₆₀ are directed normal to the surface. A total of 300 trajectories were calculated for Ga, and 83 trajectories were sampled for C₆₀. Each trajectory was initiated with a fresh sample with all atoms in their equilibrium minimum energy positions. The atoms in the target initially have zero velocity. The atoms in the C₆₀ projectile initially have no velocity relative to the center of mass motion toward the solid. The trajectory is terminated when the kinetic energy of the most energetic particle is 0.1 eV where the binding energy is 2.95 eV. In addition, we have made six test calculations with a termination energy of 0.01 eV. The calculations ran longer, but no additional ejected particles were observed. The time of each trajectory ranges between 4 and 10 ps and depends on the type of primary projectile, its impact point, and the manner in which the energy distributes within the solid. It takes approximately 40-70 h on one processor to complete a single trajectory on a 2.5-GHz Pentium computer.33

As has been reported in previous simulations, $^{20-22,34-36}$ large pressure waves are generated during cluster bombardment. When reaching the boundary of the necessarily finite simulation volume, these waves are reflected and propagate toward the surface. Thus, the reflected waves will artificially affect further evolution of the system, which may lead to unreliable results. We have extensively tested the boundary conditions and find that the qualitative character of the C_{60} bombardment on the Ag surface remains independent of the choice of boundary conditions. We have chosen one approach that is most effective at removing the reflected pressure wave.

Techniques for removing pressure waves have been developed for processes such as laser ablation.³⁷ In the laser ablation situation, there is one pressure wave that is traveling in one direction. For the C_{60} bombardment, there are several pressure waves that are traveling in different directions. Rather than develop pressure damping boundary conditions for the C_{60} bombardment, we explored the generalized Langevin equation (GLE) ap-

⁽¹⁷⁾ Webb, R. P.; Kerford, M.; Way, A.; Wilson, I. Nucl. Instrum. Methods B 1999, 153, 284.

⁽¹⁸⁾ Seki, T.; Aoki, T.; Tanomura, M.; Matsuo, J.; Yamada, I. Mater. Chem. Phys. 1998, 54, 143.

⁽¹⁹⁾ Aoki, T.; Seki, T.; Matsuo, J.; Insepov, Z.; Yamada, I. Mater. Chem. Phys. 1998, 54, 139.

⁽²⁰⁾ Colla, Th. J.; Aderjan, R.; Kissel, R.; Urbassek, H. M. Phys. Rev. B 2000, 62, 8487.

⁽²¹⁾ Colla, Th. J.; Urbassek, H. M. Nucl. Instrum. Methods B 2000, 164, 687.

⁽²²⁾ Aderjan, R.; Urbassek, H. M. Nucl. Instrum. Methods B 2000, 164, 697.

⁽²³⁾ Nguyen, T. C.; Ward, D. W.; Townes, J. A.; White, A. K.; Krantzman, K. D.; Garrison, B. J. J. Phys. Chem B 2000, 104, 8221.

⁽²⁴⁾ Garrison, B. J. In ToF-SIMS: Surface Analysis by Mass Spectrometry, Vickerman, J. C., Briggs, D., Eds.; SurfaceSpectra Ltd. & IMPublications: Manchester, U.K., 2001; p 223.

⁽²⁵⁾ Garrison, B. J.; Delcorte A.; Krantzman, K. D. Acc. Chem. Res. 2000, 33, 69

⁽²⁶⁾ Garrison, B. J. Chem. Soc. Rev. 1992, 21, 155.

⁽²⁷⁾ Kelchner, C. L.; Halstead, D. M.; Perkins, L. S.; Wallace, N. M.; DePristo, A. E. Surf. Sci. 1994, 310, 425.

⁽²⁸⁾ Stuart, S. J.; Tutein, A. B.; Harrison, J. A. J. Chem. Phys. 2000, 112, 6472.

⁽²⁹⁾ Brenner, D. W. *Phys. Rev. B* **1990**, *42*, 9458.

⁽³⁰⁾ Brenner, D. W.; Shenderova, O. A.; Harrison, J. A.; Stuart, S. J.; Ni, B.; Sinnott, S. B. J. Phys.: Condens. Matter 2002, 14, 783.

⁽³¹⁾ http://www.sesres.com/PhysicalProperties.asp.

⁽³²⁾ Postawa, Z.; Piaskowy, J.; Ludwig, K.; Winograd, N.; Garrison, B. J. Nucl. Instrum. Methods 2003, 202, 168.

⁽³³⁾ http://gears.aset.psu.edu/hpc/systems/lionxl/.

⁽³⁴⁾ Webb, R. P.; Kerford, M. Nucl. Instrum. Methods B 2001, 180, 32.

⁽³⁵⁾ Kerford, M.; Webb, R. P. Nucl. Instrum. Methods B 2001, 180, 44.

⁽³⁶⁾ Haberland, H.; Isepov, Z.; Moseler, M. Phys. Rev. B 1995, 51, 11061.

⁽³⁷⁾ Zhigilei, L. V.; Garrison, B. J. In Multiscale Modelling of Materials; Diaz de la Rubia, T., Kaxiras, T., Bulatov, V., Ghoniem, N. M., Phillips, R., Eds.; Materials Research Society Symposia Proceedings 538; Materials Research Society: Warrendale, PA, 1999; p 491.

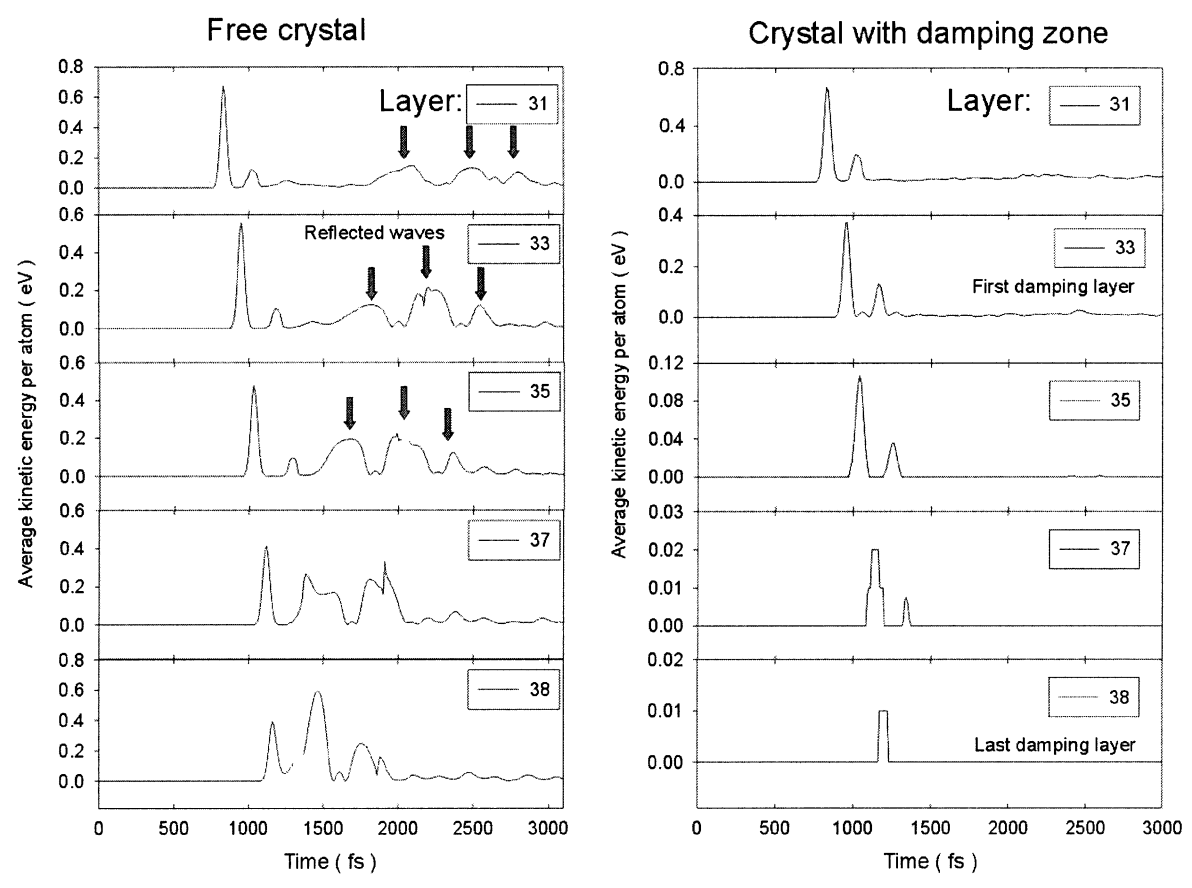


Figure 1. Time dependence of the average kinetic energy of silver atoms as a function of depth for a 20-keV C_{60} projectile for simulations with free boundaries and the damping boundaries described above. The zone interface occurs between layers 32 and 33. The average kinetic energy is calculated for atoms located in a 12 \times 12 \times 5 Å box placed at various depths directly under the center of mass impact point of the 20-keV C_{60} cluster bombarding Ag{111} surface.

proach. 38,39 In the limit of 0 K, this approach is similar to those used in other cluster bombardment simulations. ^20,21,40,41 The GLE approach is physically correct only for thermally equilibrating the system with an infinite heat bath, but since it does remove energy at the boundary of the crystallite, there is the potential for it to handle low-energy pressure waves as well. In this approach, the solid is divided into three zones. The first zone contains atoms that move according to Newtonian equations of motion with the interaction potentials described above. This zone is surrounded by atoms with additional Langevin (frictional) forces. The movement of atoms, six layers thick in our simulation, in the second zone is damped proportionally to their velocities, causing the energy from the pressure wave to be extracted. Finally, the system is surrounded on five sides by a layer of rigid atoms. We used a damping constant proportional to the substrate Debye temperature^{38,39} and a Debye temperature of 215 K.⁴²

The time dependence of the average kinetic energy of silver atoms as a function of depth for a 20-keV C_{60} projectile is shown in Figure 1 for simulations with free boundaries and the damping boundaries described above. The zone interface occurs between layers 32 and 33. It is clearly visible that three pressure waves

develop in the bombarded solid. All these waves reflect from the boundaries of the free crystal and start propagating upward at \sim 2 ps. The speed of the returning pressure wave is less as there is considerable distortion at the bottom of the free crystal; thus, the material properties are not the same as the initial sample.³⁷ In the crystal with a damping zone, however, the energy of the pressure wave is absorbed and minimal reflection is present. The total average energy removed for 20-keV C_{60} bombardment is ~ 5.7 keV. Although the majority of the energy is removed, there does remain a small, reflected pressure wave. The application of the damping zone reduces the total sputtering yield by \sim 7% for 20keV C_{60} and \sim 3% for 15-keV C_{60} as compared with the simulation with the free boundaries. Finally, it should be pointed out that the proposed protocol for damping boundary conditions cannot be used for sputtering induced by a high-energy monomer projectile.²⁴ In this case, the maximum kinetic energy of individual particles when they reach the sides or the bottom of the sample can be thousands of electronvolts. The applied damping zone would not be able to absorb this amount of energy, and a strong reflection of energy at the zone interface will be present. Fortunately, bombardment by the monomer projectile does not lead to the generation of pressure waves; thus, open boundary conditions are used in this case.24

RESULTS AND DISCUSSION

Cross sectional views of the temporal evolution of typical collision events leading to ejection of atoms during 15-keV C_{60}

⁽³⁸⁾ Adelman, S. A.; Doll, J. D. J. Chem. Phys. 1974, 61, 4242.

⁽³⁹⁾ Garrison, B. J.; Kodali, P. B. S.; Srivastava, D. Chem. Rev. 1996, 96, 1327.

⁽⁴⁰⁾ DePristo, A. D.; Metiu, H. J. Chem. Phys. 1989, 90, 1229.

⁽⁴¹⁾ Moseler, M.; Nordiek, J.; Haberland, H. Rhys. Rev. B 1997, 56, 15439.

⁽⁴²⁾ Ashcroft, N. W.; Mermin, N. D. Solid State Physics; Saunders College Publishing: Orlando, FL, 1976.

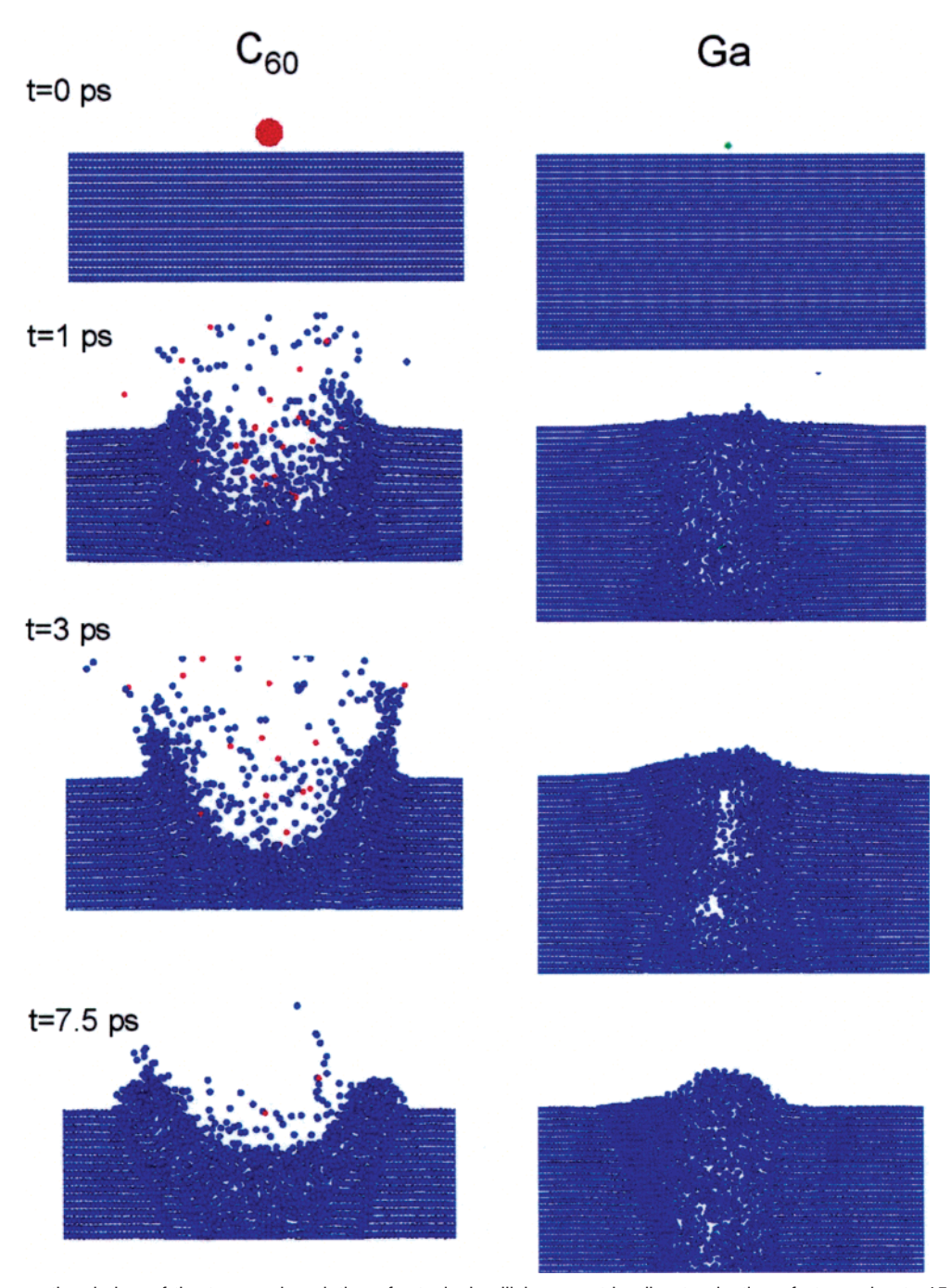


Figure 2. Cross sectional view of the temporal evolution of a typical collision event leading to ejection of atoms due to 15-keV C60 and Ga bombardment of a Ag{111} surface at normal incidence. Blue, red, and green depict silver, carbon, and Ga atoms, respectively.

and Ga bombardment are shown in Figure 2. It is clearly visible that the collision cascades initiated by C₆₀ and Ga projectiles are different. As described also by Yamada and co-workers for C60 bombardment on diamond, 19 the C_{60} projectile dissociates upon impact and most of the carbon atoms are backscattered into the vacuum. The impact leads to formation of numerous superimposing cascades that highly disorder a relatively shallow volume of the crystal below the surface in a very short time. This dense, liquidlike region closes off open channels so that individual carbon atoms cannot penetrate deep into the sample. As a consequence, a significant amount of the projectile's energy is deposited close to the surface, leading to the emission of many particles. In addition, as is visible in Figure 1, immediately after the impact,

pressure waves are generated in the solid. Both the ejection of atoms and the propagation of the pressure pulse are driving forces for a crater formation. Consequently, a deep, roughly hemispherical crater surrounded by a huge rim is formed. This crater formation is almost macroscopic in nature and only weakly depends on the initial impact point of the C₆₀ molecule on the surface.

Since the C₆₀ projectile creates a crater in the surface, we paid special attention to the definition of ejection. Particles, both atoms and clusters, are considered to be ejected if they are at a distance larger than 20 Å from the original surface plane, they do not interact with anything else, and they have a velocity vector directed toward the vacuum. The boundary line is higher than the position

Table 1. Total Sputtering Yield and Number of Particles Emitted from 15-keV C₆₀ and Ga Bombarded Ag{111} Surface at Normal Incidence Per Single Projectile^a

	projectile	
	C ₆₀	Ga
total sputtering yield	331.0	21.0

	no. of eject per single	no. of ejected particles per single projectile	
particle	C ₆₀	Ga	
all	171.5	17.3	
Ag	102.7	15.0	
$egin{array}{c} Ag \\ Ag_2 \end{array}$	44.2	1.8	
Ag_3	11.6	0.33	
Ag ₄	4.5	0.09	
Ag_5	2.4	0.01	
$egin{array}{c} { m Ag}_5 \ { m C} \end{array}$	53.2		
Ga		0.06	

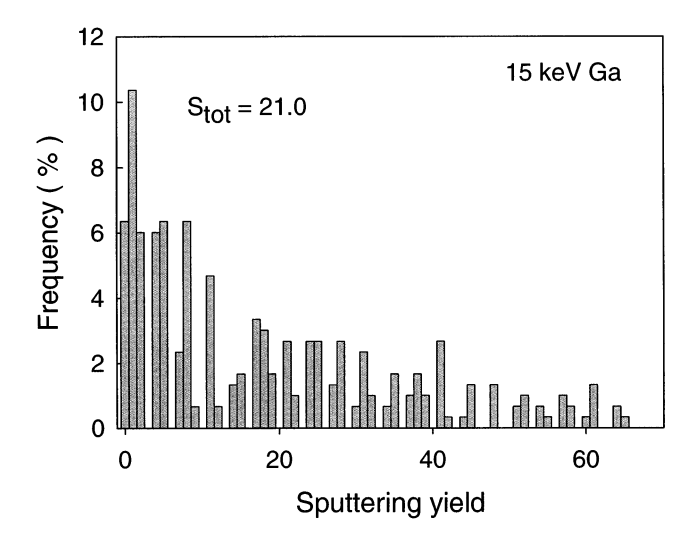
^a Number of backscattered projectile atoms is also given. In both cases, larger clusters are omitted from the table; thus, the sum of the yields of individual species does not sum to the total sputtering yield.

at which adatoms are finally located. Obviously, during "eruptions" it is possible that some of the atoms in the side jets cross the boundary line, but since they interact with the crystal (through other atoms in the jet), they are not treated as sputtered. All atoms visible below the surface at Figure 2 at 7.5 fs have velocity vectors directed toward the pit. This particular trajectory terminates at 8.7 ps.

A different type of movement is visible for 15-keV Ga. The cascade presented in Figure 2 results in emission of 21 particles, which is close to the average sputtering yield induced by 15-keV Ga. The monomer projectile penetrates deeper into the crystal as compared to C_{60} bombardment, and the damaged area has more cylindrical rather than hemispherical symmetry. There is a significant amount of movement, but it occurs deep under the surface. The movement leads to a creation of a large void in the crystal. Particles located in the topmost two to three layers are mostly ejected. At the same time, a significant number of deeper lying atoms are ejected during C_{60} bombardment.

A critical difference in the two projectiles is the size of the species. The diameter of C_{60} is \sim 7 Å while Ga projectile has a diameter of only 1.3 Å. As a result, many Ga projectiles penetrate deep into the crystal before any collision with a Ag atom takes place. As a consequence, a significant amount of primary energy will be buried deep in the crystal and only a small portion of this energy will be deposited in the vicinity of the surface and cause sputtering. The dynamics of the larger projectile is more macroscopic in nature rather than based on atomic collisions; thus, in hindsight, it is not surprising that craters form for graphite $^{17.18}$ and diamond 19 substrates as well as for Au₄ bombardment of graphite 17 and gold. $^{20.21}$

The total sputtering yield is given in Table 1. The total yield is almost 16 times larger for C_{60} than for Ga bombardment. Yield enhancements during cluster bombardment are well known and have been observed both in calculations, see for example refs 20-22 and 43, and in experiment, see for example, refs 44-46.



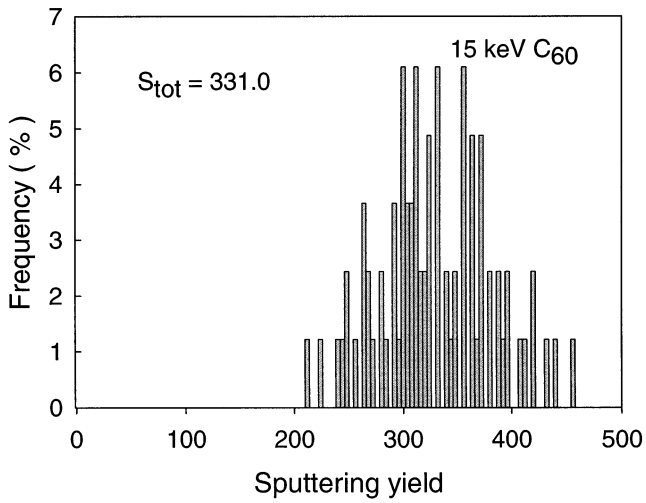


Figure 3. Relative frequency of impacts leading to a given sputtering yield for 15-keV Ga and C_{60} projectiles on a Ag{111} surface at normal incidence.

The difference in behavior of the systems bombarded with 15-keV Ga and C_{60} projectiles is reflected in the relative frequency of impacts leading to ejection of a total number of silver atoms in monomers and clusters as shown in Figure 3. Each impact of C_{60} cluster leads to very efficient emission, whereas a significant number of Ga impacts terminate without any ejection. This small deviation in yield for C_{60} bombardment with impact point is consistent with the visual observation that all motions in the solid look similar.

In SIMS and postionization experiments, the total yield of material removed is not generally measured. Rather, the average numbers of individual species such as monomers, dimers, and larger clusters are recorded. The average number of the various ejected particles is shown in Table 1 to enable a more direct comparison of our data to the results obtained in experiment. For

⁽⁴³⁾ Betz, G.; Husinsky, W. Nucl. Instrum. Methods B 1997, 122, 311.

⁽⁴⁴⁾ Heinrich, R.; Wucher, A. In Atomic Collisions in Solids; Ellegard, O., Møller, S. P., Schou, J., Sigmund, P., Eds.; Elsevier Science: New York, 2000; p 720.

⁽⁴⁵⁾ Andersen, H. H.; Bay, H. L. J. Appl. Phys. 1974, 45, 953, Andersen, H. H.; Bay, H. L. J. Appl. Phys. 1975, 46, 2416.

⁽⁴⁶⁾ Andersen, H. H.; Brunelle, A.; Della-Negra, S.; Depauw, J.; Jacquet, D.; Le Beyec, Y; Chaumont, J.; Bernas, H. Phys. Rev. Lett. 1998, 80, 5433.

15-keV C_{60} and Ga, the ratio of total sputtering yields is \sim 16, while the ratios of monomer, dimer, and trimer yields are 7, 25, and 35, respectively. The enhancement of various species is clearly different. Such behavior can be expected based on the snapshots of the atomic motions shown in Figure 2. The development of a collision cascade immediately following impact exhibits a large density of energy deposited in subsurface volume by C₆₀ bombardment, and large chunks of material are ejected at the early stages of development of collision cascade. In addition, at the later stages, a large number of slowly moving atoms enclosed near the base of the crater have the potential to favor more abundant cluster emission. A similar effect of cluster enhancement has been observed in the gold cluster bombardment studies²⁰ and experiments of Ag clusters bombarding silver substrates. 44 Experiments are underway to measure the yield of the various species with Ga⁺ and C₆₀⁺ bombardment.⁴⁷

CONCLUSIONS

The MD simulations clearly demonstrate that C_{60} projectiles can initiate crater formation even in heavy metal substrates such as Ag in the same manner as Au_4 projectiles striking metal substrates^{20,21} and C_{60} bombardment on graphite^{17,18} and diamond.¹⁹ The cluster beam is able to deposit significant energy in the near-surface region that gives rise to the increased ejection. Moreover, the energy that penetrates deep into the substrate is

in a pressure wave that does not induce significant atomic displacements and damage.

The results presented in this paper deal with the processes taking place on clean metal surfaces. Important predictions, however, can also be drawn for C_{60} bombardment of thin organic overlayers deposited on metal substrates. Simulations performed for organic overlayers on metal substrates show that collective action of several substrate atoms is required to eject large organic molecules. 25,48 Irradiation by C_{60} clusters should enhance molecular emission due to the occurrence of the large collective motions involved. In addition, the issue of damage remaining in the near-surface region could be critical for applications of depth profiling of organic and biological materials. Simulations of C_{60} bombardment of thin and thick overlayers of organic molecules on metal substrates are underway.

ACKNOWLEDGMENT

Financial support from the Polish Committee for Scientific Research, CYFRONET, National Science Foundation, and the National Institutes of Health are gratefully acknowledged. The Academic Services and Emerging Technologies group at Penn State provided us early access to the lion-xl PC cluster. We appreciate helpful discussions with Andreas Wucher.

Received for review April 14, 2003. Accepted June 9, 2003.

AC034387A

⁽⁴⁷⁾ Wucher, A.; Sun, S.; Szakal, C. W.; Winograd, N., unpublished.

⁽⁴⁸⁾ Delcorte, A.; Garrison, B. J. J. Phys. Chem. B 2000, 104, 6785.